DOI: 10.1002/cmdc.200800259

How to Extend the Use of Grid-Based Interaction Energy Maps from Chemistry to Biotopics

Giulia Caron, Alessandra Nurisso, and Giuseppe Ermondi*[a]

*Many computational tools routinely used in chemistry could successfully be applied to the biosciences since protein–protein and protein–ligand interactions are governed by the laws of chemistry. This paper shows that it is possible to extend the use of existing computational tools from their traditional application field (*e.g. *chemistry) to culturally-related research areas by the implementation of simple but well-designed utilities. In particular, a computational strategy obtained by combining GRID (the program originally designed by Peter Goodford, and now distributed by Molecular Discovery Ltd.) and BIOCUBE4mf (an application freely available at* www.casmedchem.unito.it*) was used to a) characterize the surface properties of the cavity of the* Bacillus anthracis *protective antigen heptameric prepore; b) suggest how to design mutagenesis experiments; c) quantitatively show the selectivity of the KvAP channel for K^+ over Na^+ ions and d) rationalize the pharmacokinetic behavior of 1,4-DHP third-generation drugs.*

Introduction

Nowadays, it is evident that a number of biology-related disciplines (medicinal chemistry, pharmaceutical sciences, chemoinformatics, bioinformatics, biochemistry, pharmacology, etc.) overlap considerably. For this reason, collaboration among scientists working in these fields, and the sharing of information and tools is essential.

Biosciences and crystallography have a strong tradition in terms of freely-available resources, whereas chemists are rather more reluctant to share their skills with other scientists.[1,2] This cultural tendency to reject the challenge of multidisciplinary tends to isolate chemists from other researchers with different backgrounds, as is shown by the fact that, for example, chemistry and bioinformatics often concern the same topic while adopting different viewpoints and vocabularies. We have already discussed this difficulty in communication in a previous paper, using recognition forces in ligand–protein complexes as an example.[3] Nevertheless, many computational resources developed by chemists are of potential interest to researchers working in different scientific areas.[4]

This study was undertaken to show how a simple, well-designed application can get the most out of a typical computational chemical resource, extending the use of currently-available tools from chemistry to biosciences. In particular, the paper describes a computational strategy aimed at extracting the most information from grid-based interaction energy maps, using GRID and BIOCUBE4mf as an example. GRID (Windows version 22 b, http://www.moldiscovery.com) was originally designed by Peter Goodford and is now distributed by Molecular Discovery (see Supporting Information for a brief summary of the theory) and BIOCUBE4mf (version 1.1.0, freely available at www.casmedchem.unito.it, see Supporting information for more details), developed in our laboratory, is a simple but essential tool that enables the interpretation of GRID outputs in more practical terms.

The results of the application are illustrated through four examples covering a wide range of chemical and biochemical topics: a) characterization of the surface properties of the *Bacillus anthra*cis protective antigen heptameric prepore cavity; b) rationalization of mutagenesis experiments applied to the cytosolic sulfotransferase (SULT) superfamily; c) investigations of the potassium channel (KvAP) selectivity; and d) study of the pharmacokinetic relevance of the surface features of some 1,4-dihydropyridine (1,4-DHP) third-generation drugs.

Discussion

BIOCUBE4mf: an example of a "bridge" between chemistry and neighboring disciplines

As outlined in the Introduction, the growing overlap of scientific disciplines calls for a strong collaboration among researchers. However, researchers often meet with difficulties in communication, consequently ad hoc tools are required to enable concepts to be transferred among different disciplines to produce improvements in research activities. BIOCUBE4mf is the first tool specifically designed and implemented to overcome difficulties in communications between scientists working in neighboring fields since it extracts the most relevant information from a chemical resource of huge potential, such as GRID (one of the most powerful software packages available to pro-

[a] *Prof. G. Caron, Dr. A. Nurisso, Prof. G. Ermondi*
CASMedChem Laboratory
Dipartimento di Scienza e Tecnologia del Farmaco, Università di Torino
Via P. Giuria 9, I-10125 Torino (Italy)
Fax: (+39) 011 670 7687
E-mail: giuseppe.ermondi@unito.it

Supporting information for this article is available on the WWW under http://dx.doi.org/10.1002/cmdc.200800259.

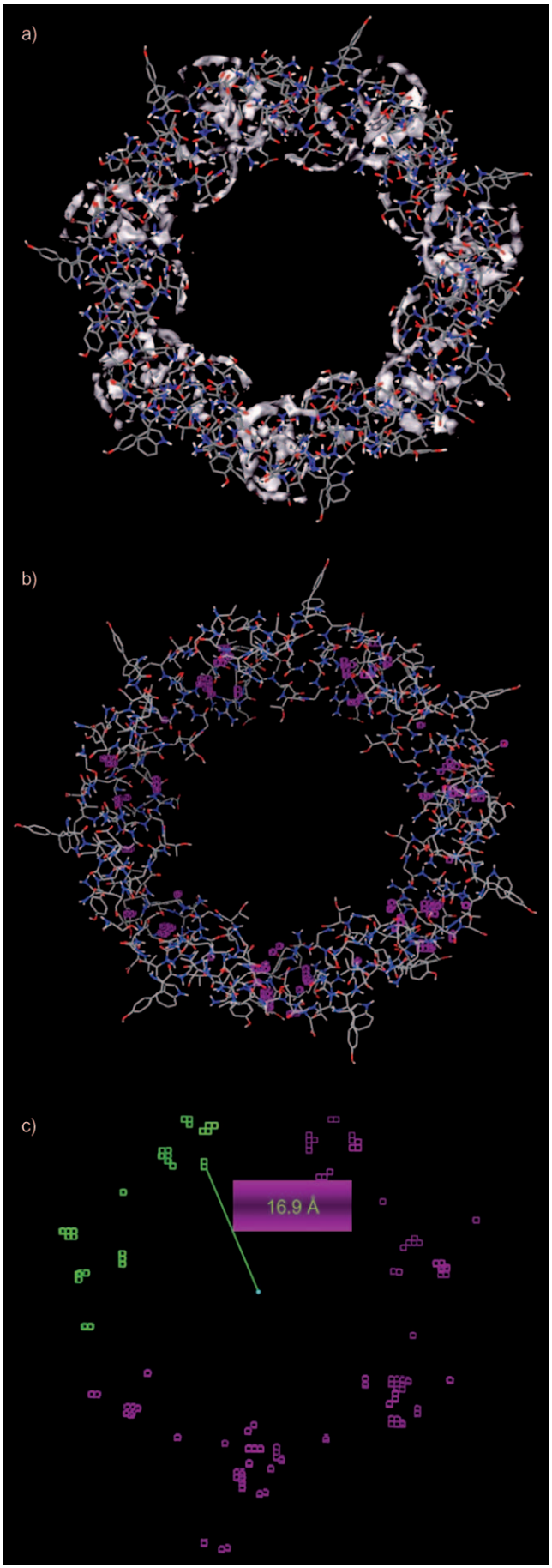

duce grid-based energy maps), and makes them of practical use to bioscientists.

Figure 1a shows an example of grid-based energy maps as visualized by GVIEW, the application used (GRID version 19 onwards) to visualize MIFs (Molecular Interaction Fields) together with (macro)molecular targets, for the *B. anthracis* protective antigen heptameric prepore cavity, using the potassium ion (K^+) as a probe. The light pink areas in Figure 1a are the isosurfaces joining all points having an interaction energy value with the K^+ probe of -9.0 kcal mol^{-1}. This is a nice graphical representation, but how useful is it in practice for research purposes? BIOCUBE4mf is the answer to this question.

Firstly, BIOCUBE4mf converts the GRID output (light pink regions in Figure 1a) to a pdb file that can be read by most molecular modeling software. This result cannot be underestimated; the comparative visual inspection of the results through superposition of molecules and interaction fields plays a key role among bioscientists.

Secondly, BIOCUBE4mf distinguishes the main from the additional information present in a GRID output through a simple points clusterization technique. Despite the simplicity of the method, the presence of these clusters allows identification and selection of regions where relevant interactions occur. The size and relative distances of these interaction regions can be obtained by using different probes, BIOCUBE4mf can then easily assemble a complete map of interaction pattern.

Finally, BIOCUBE4mf quantitatively evaluates the estimated volume of the selected clusters, and lists the results in an ASCII file. In particular, BIOCUBE4mf identifies the number of points below a certain energy value. This operation appears trivial, but in practice it is the only way to select a reasonable energy level, using the number of MIF points as criterion through which to study the investigated topic. The choice of energy cut-off values is in fact a major problem in energy-based grid maps, since no general rule exists to select the cut-off value owing to the close dependency of this value on the structure investigated. Moreover, with the multifile option, it is possible to compare two or more MIFs by the calculation of some well-known similarity/dissimilarity indexes, for example, Tanimoto, Carbo, Hodgkin, etc.[5]

Results obtained by applying the GRID/BIOCUBE4mf strategy to four selected examples spanning a wide range of chemical and biological topics are discussed below. These applications were chosen to demonstrate the versatility of the method, which can be applied to a variety of research fields.

Figure 1. The zone around the *B. anthracis* protective antigen heptameric prepore cavity (see test for details) The prepore cavity was limited by selecting those amino acids that show a distance from the centroid of less than 25 Å. (pdb code: 1TZO, missing amino acids were not added since they were not necessary for this study). K^+ probe is used. a) Visual representation as provided by GVIEW (NPLA = 1.5). b) Visual representation as provided by BIOCUBE4mf, visualized by MOE. c) Visual representation as provided by BIOCUBE4mf, visualized by MOE, but the clusters generated by BIOCUBE4mf and due to one subunit are in green. The distance from one point of the cluster and the centroid is also shown.

Characterization of the surface properties: the case of *B. anthracis* protective antigen heptameric prepore

B. anthracis, the organism causing anthrax, is potentially one of the most dangerous biological weapons. The protective antigen (PA) is the central component of the three-part protein toxin secreted by *B. anthracis*. After binding to cell receptors and proteolytic activation, PA forms a heptameric prepore, which then undergoes pH-dependent conversion to a pore, mediating translocation of the edema and lethal factors to the cytosol.[6] Blockage of the prepore/pore by a small molecule could inhibit the mechanism of action of the anthrax toxin. The design of an ad hoc prepore/pore blocker requires a detailed understanding of the chemical features of the PA cavity, which is expected to be negatively charged.[7] The crystal structure of the *B. anthracis* protective antigen heptameric prepore was taken from the PDB database (pdb code: 1TZO), and GRID (Windows version 22 b, http://www.moldiscovery.com) calculations were run using K^+ as a probe. Results found by GVIEW are shown in Figure 1 a, where the isosurfaces joining all points having a favorable interaction energy value with the K^+ probe (threshold cutoff: -9.0 kcal mol^{-1}) are shown in light pink. Figure 1 a shows that the interactions of the probe with the pore are localized to particular regions; characterization of these regions may provide insight into the interactions. Figure 1 b shows cubes and clusters obtained by BIOCUBE4mf, which required ~30 sec to generate Figure 1 b from Figure 1 a. Figure 1 c illustrates one of the main features of BIOCUBE4mf, which enables the user to select one or more clusters at a time, or in other words, to separate clusters of greater interest from the others. As an example, in Figure 1 c we selected those clusters due to a monomeric subunit (green), and calculated the distance from the centroid of the whole protein for one of them (16.9 Å). The results can be applied to design new prepore blockers with precise chemical features.

The crystal structure of the anthrax toxin protective antigen heptameric prepore was downloaded from PDB database (pdb code: 1TZO). Missing amino acids were not added since they were not necessary for this study. The prepore cavity was limited by selecting those amino acids that show a distance from the centroid of less than 25 Å. GRID calculations were run using NPLA = 1.5 and the phosphate dianion (PO_4^{2-}) as a probe.

Designing mutagenesis experiments

Members of the cytosolic sulfotransferase (SULT) superfamily catalyze the sulfation of a multitude of xenobiotics, hormones and neurotransmitters.[8] The protein folds of the SULT enzymes whose structures have been solved are essentially superimposable; however, some subtle but important differences in the active sites do exist. The human SULT 1A3 enzyme, for example, displays a high selectivity for endogenous and xenobiotic catecholamines (particularly dopamine) not shared by its close relative SULT 1A1, even though the two enzymes are more than 93% identical at the amino acid sequence level (i.e. only 20 out of 295 residues differ). Analysis of these sequence differences showed that a number of them occur close to one another (residues 143–152). Mutation of two amino acids in this section of the SULT 1A3 protein to the corresponding SULT 1A1 residues (His 143 → Tyr and Glu 146 → Ala) clearly demonstrated that Glu 146 was the major determinant of the specificity of SULT 1A3 for dopamine. Moreover, the influence of Glu 146 probably controls the orientation of many compounds in the SULT 1A3 active site, explaining the selectivity of SULT 1A3 for catechols over the corresponding phenols.

Given these findings, we studied the differences introduced by the two mutations (His 143 → Tyr and Glu 146 → Ala) into the original 3D structures of SULT 1A3, employing a different approach rather than the traditional visual inspection of the interactions formed with the substrate (either crystallized or docked). After downloading SULT 1A3 from the protein database, this and the corresponding mutated structures were submitted to GRID. The neutral flat NH amide (N1) and carbonyl oxygen (O) probes were used to monitor the hydrogen bonding (HB) pattern. GRID output files (.lont and .kont) were then used as input for BIOCUBE4mf, and the following energy cutoffs were chosen: -8.5 kcal mol^{-1} (N1) and -7.0 kcal mol^{-1} (O). The SIMI option in BIOCUBE4mf gave the results shown in Table 1; the crystallographic structure has greater similarity with the 143 mutant than with that 146 mutant (Tanimoto indexes 0.916 and 0.881, respectively). In other words, BIOCUBE4mf analysis clearly indicates that mutation at position 146 alters the HB pattern of the active site more profoundly than mutation of the 143 residue.

Table 1. Numerical output obtained from BIOCUBE4mf: Data obtained by BIOCUBE4 mf (N1 probe) to characterize mutagenesis studies on SULT 1A3.

3D structure		Tanimoto index[a]	Hodgkin index[a]
A	B		
SULT 1A3[b]	SULT 1A3_143[c]	0.916	0.956
SULT 1A3	SULT 1A3_146[d]	0.881	0.937
SULT 1A3_143	SULT 1A3_146	0.806	0.893

[a] The Tanimoto and Hodgkin indexes refer to the couple of structures in columns A and B. Dimensions of the GRID box were: X+39.8:+53.3; Y+106.8:+120.3; Z-11.3:+22.2. The parameter NPLA was set to 2.0. [b] Original 3D structure (pdb code: 2A3R). [c] Mutation in position 143. [d] Mutation in position 146.

The relevance of this finding in the design of mutagenesis studies is evident, given the widespread and increasing use of this technique to investigate the role of individual amino acids implicated in ligand binding or signal transduction. The choice of the "best" mutation for a given amino acid is not a trivial problem, as is shown by an examination of the literature. As an example, while some studies use alanine to replace putative residues and prove their importance in the functionality profile of the protein, since its lateral chain is small and thus in principle not able to alter the secondary structure of the protein, other studies prefer to test a number of residues bearing side chains of different lengths, charges or bulky groups leading to steric hindrance. Moreover, it is common practice to replace

hydrophobic amino acids with hydrophilic residues when investigating the oligomerization properties of a peptide, though no definitive rule has ever been proposed to further explain this connection. With the GRID/BIOCUBE4mf strategy, it is possible to check how much the replacement may alter the original structure through analysis of simple numerical indices, which refer to a sophisticated background analysis.

The X-ray structure of SULT1A3 was obtained from the protein database (pdb code: 2A3R). The corresponding mutated structures were obtained using the ad hoc tool, rotamer explorer, implemented in MOE (Version 2007.09, Chemical Computing Group Inc., Montreal, Canada).

Potassium ion channel selectivity

Potassium ion channels are transmembrane proteins that serve a wide range of important physiological functions, most of which rely on the ability of the channel to allow K^+ to permeate, but not the smaller and more abundant Na^+ ion.[9] Given this situation, we reasoned that selectivity could also be investigated using the GRID/BIOCUBE4mf strategy using K^+ and Na^+ as probes. Indeed, maps like that shown in Figure 1c, can also be calculated for the KvAP channel and, in principle, results obtained with the K^+ probe should be different from the correspondent results obtained with Na^+.

As before, GRID output files (.lont and .kont) were then used as input for BIOCUBE4mf, and a preliminary energy cutoff of -20 kcal mol^{-1} was chosen, so as to obtain a rough indication of the numerical results. Figure 1a and the data listed in Table 2 appear to suggest that a) the channel pore in proximity to the potassium selectivity filter (characterized by the well-known sequence motif Thr–Val–Gly–Tyr–Gly) is, as expected, the region in which the highest concentration of cubes is located and b) KvAP preferably interacts with Na^+ rather than with K^+ ions. The obvious absurdity of this second result was probably due to the fact that -20 kcal mol^{-1} is too high a cut-off value, and thus not sufficiently selective. The energy cut-off was lowered, and different values were tested (Table 2). The numerical results are intriguing, since they show that, in an energy range of -20 to -45 kcal mol^{-1}, the number of cubes and clusters arising due to K^+ is relatively constant, whereas for Na^+ the number of cubes decreases markedly, while the number of clusters increases. Finally, at an energy cut-off of -48 kcal mol^{-1}, MIFs due to the Na^+ ion did not allow formation of any cube (nor therefore of any clusters). These data are represented graphically in Figure 2b–e, showing the selectivity of the KvAP channel for K^+ over Na^+ ions (all BIOCUBE4mf calculations were performed in ~1 min). Additional proof of the reliability of the results is given in Figure 3, which clearly shows that the calculated cubes (in white) mainly coincide with two experimental known potassium sites (P2 and P3), and are in line with the remaining four (P1, P4, P5 and P6) of the original X-ray structure. The relevance of this result can readily be confirmed by using it to validate the results of homology modeling results. Briefly, once a number of structurally reliable 3D protein models have been generated (i.e. without any inconsistency), the ability of these models to reproduce K^+ over Na^+ selectivity can be quantified by the GRID/BIOCUBE4mf technique, and the numerical values used to rank models for their "physiological" relevance.

Table 2. Numerical output obtained from BIOCUBE4mf: MIFs data as calculated by BIOCUBE4mf to describe KvAp channel selectivity for potassium versus sodium ions.

Energy cut-off [kcal mol^{-1}]	Probe K^+		Probe Na^+	
	Cubes	*Clusters*	*Cubes*	*Clusters*
−20	44	14	87	17
−25	16	2	62	1
−30	15	1	39	2
−35	10	1	32	2
−40	10	1	16	2
−45	10	1	8	3
−48	9	1	0	0

Finally, to illustrate another BIOCUBE4mf feature that would be of great interest to many bioscientists, Figure 4a analyzes the previously-mentioned sequence motif Thr–Val–Gly–Tyr–Gly of the potassium channel selectivity filter[9] using an N1 probe (-3.0 kcal mol^{-1}) to verify the hydrogen bond acceptor properties of the amino acid sequence. It might then be of interest to visualize the contribution of the hydroxyl moiety of the lateral Tyr chain alone, since it is outside the channel filter. This can be achieved in two different ways, and the results are shown in Figure 4a and b. In Figure 4a, after visualizing the whole set of selected points in dark grey, those at a given distance (3.5 Å) from the phenolic oxygen atom were determined by MOE tools and colored in black. In Figure 4b, the same procedure was applied to the cubes.

The X-ray structure of the voltage-dependent potassium channel, KvAP, of *Aeropyrum pernix* was obtained from the protein database (pdb code: 1ORQ). Starting from the monomer coordinates, the symmetry operators present in the pdb file were used to obtain the entire fourfold symmetric structure of the pore with MOE. Dimensions of the GRID box were: X-15:+15; Y-15:+15; Z+21:+71, the NPLA parameter was set to 1.5 and the K^+ and Na^+ probes were used.

The peculiar pharmacokinetic behavior of 1,4-DHP third-generation drugs

GRID/BIOCUBE4mf can also be applied to small molecules. Here we discuss the relevance of our computational strategy in rationalizing the peculiar pharmacokinetic behavior of two calcium channel antagonists, amlodipine and lercanidipine (Figure 5a–d). The 1,4-dihydropyridines (1,4-DHPs) are a well-known class of calcium channel antagonists, used to treat hypertension. Amlodipine and lercanidipine belong to the third generation of 1,4-DHPs, characterized, in terms of their pharmacokinetics, by their prolonged effect (long clinical half-life).[10,11] The long-lasting action of these compounds is ascribed to their strong affinity for cell membranes, confirmed by their elevated membrane partition coefficient $D^{7.0}_{mem}$ (log $D^{7.0}_{mem}$ is

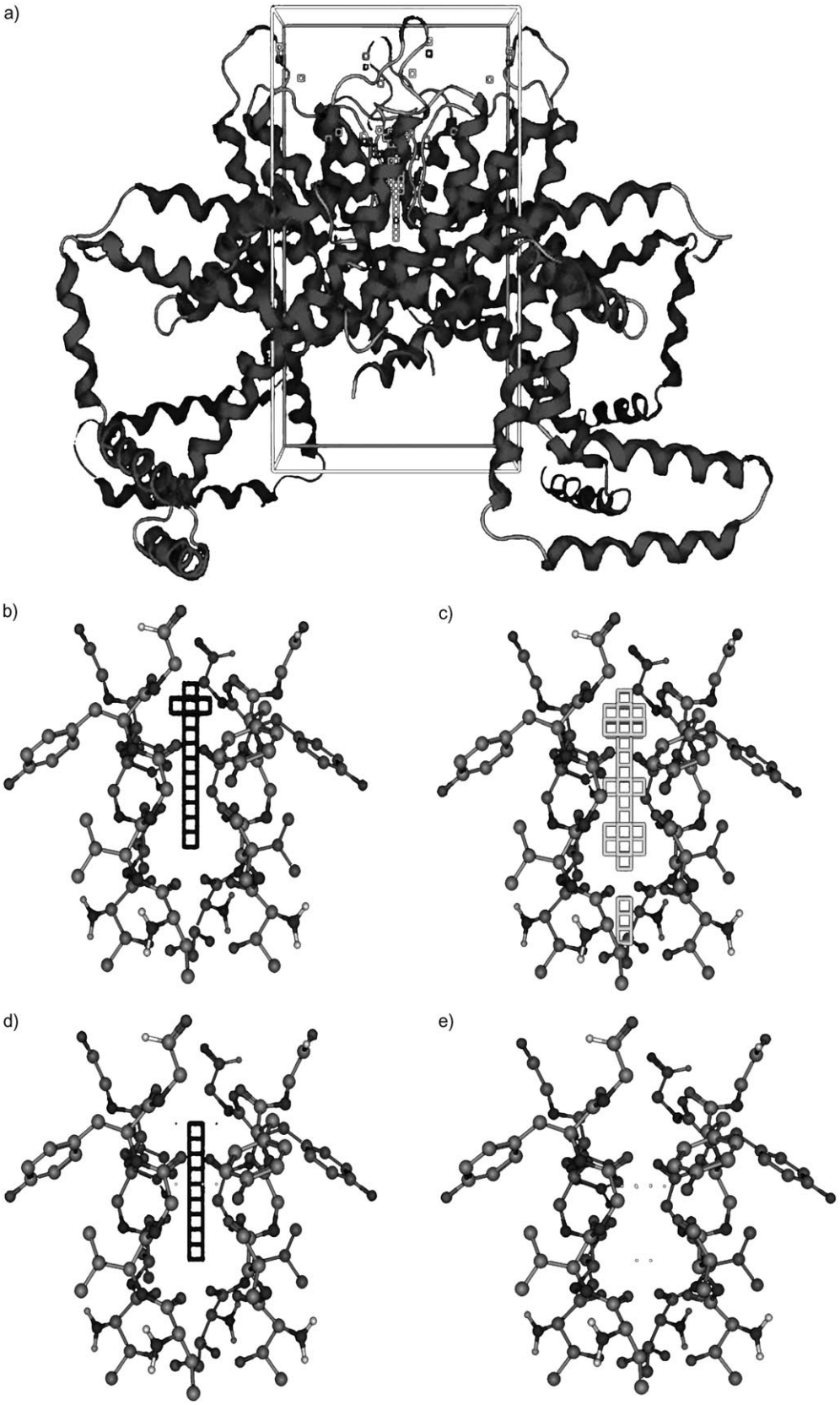

Figure 2. The X-ray structure of the voltage-dependent potassium channel KvAP (pdb code: 1ORQ). a) The four subunits comprising the tetrameric channel are shown; together with the cubes obtained from BIOCUBE4mf (grey for those extracted from MIF calculated using the Na^+ probe at -30 kcal mol^{-1} and black for the MIF due to the K^+ probe at the same energy cutoff). GRID box is also shown in grey. b) The selectivity filter (Thr–Val–Gly–Tyr–Gly) of the KvAP channel: two of the four subunits are shown, together with cubes extracted from the MIF calculated using the K^+ probe at -30 kcal mol^{-1}. c) The selectivity filter with cubes extracted from the MIF calculated using the Na^+ probe at -30 kcal mol^{-1}. d) The selectivity filter with cubes extracted from the MIF calculated using the K^+ probe at -48 kcal mol^{-1}. e) The selectivity filter with points (no cube was found) extracted from the MIF calculated using the Na^+ probe at -48 kcal mol^{-1}.

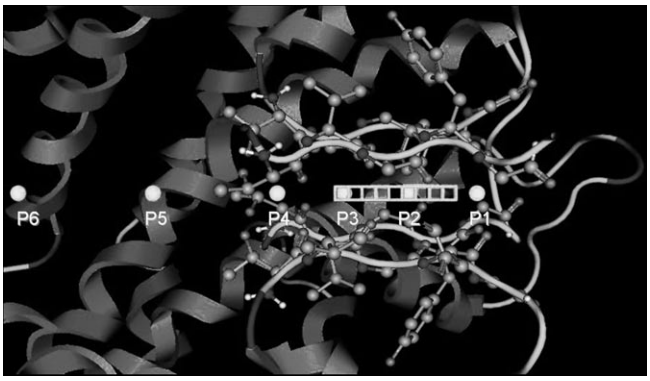

Figure 3. Comparison between BIOCUBE4 mf/GRID results and X-ray data. The residues forming the selectivity filter of the KvAP channel (two subunits) are in balls and sticks, the cubes as in Figure 2 d and experimental (= crystallographic) potassium ions (P1-P6) in white balls.

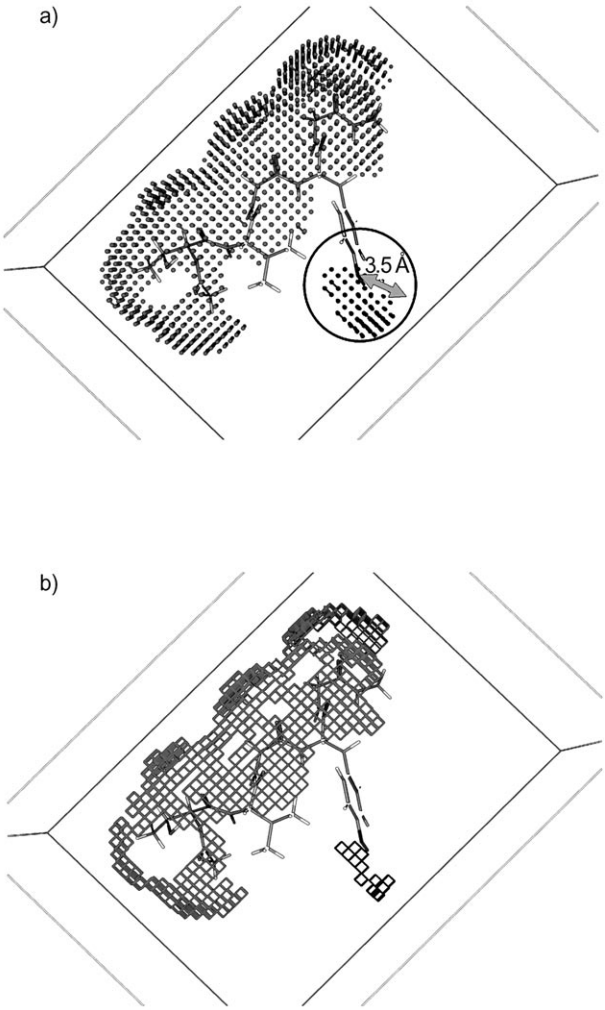

Figure 4. The sequence motif Thr–Val–Gly–Tyr–Gly of one of the four subunits of the potassium channel selectivity filter was analyzed, using the N1 probe (-3.0 kcal mol^{-1}) to detect hydrogen bond acceptor properties (grey). The contribution of Tyr alone as obtained by BIOCUBE4 mf is shown in black. a) points. b) cubes.

5.5 and 4.3 for lercanidipine and amlodipine, respectively[10]), which in turn is mainly due to two chemical features: a) high hydrophobicity and b) presence of a protonated nitrogen (lercanidipine, $pK_a = \sim 7.5$; amlodipine, $pK_a = \sim 9$[12]). An elevated molecular hydrophobicity enables the formation of hydrophobic interactions between the drug and the apolar chains of membrane phospholipids, whereas the presence of a positive charge allows ionic interactions to occur with the phosphate moieties of the phospholipids.[13] The clinical half-lives of amlodipine and lercanidipine are due to two different phenomena; a short plasma half-life for lercanidipine and a long plasma half-life for amlodipine. These two phenomena are probably due to a different balance of the two interaction mechanisms governing membrane affinity. In particular, for amlodipine the electrostatic contribution is expected to dominate over the hydrophobic interaction, whereas for lercanidipine the reverse is expected, and this fact cannot only be ascribed to the different percentage of ionized species at pH 7.0. The presence of ionic interactions might enable amlodipine to remain in the plasma compartment by linking to ionic groups located on the membrane, whereas hydrophobic interaction could enable lercanidipine to accumulate in the smooth muscle cell membranes, where calcium channels are located. To quantify the different ratios of hydrophobic and ionic interactions for the two drugs, we applied the GRID/BIOCUBE4mf strategy using two different probes, the DRY probe to mimic hydrophobic interactions and the PO_4^{2-} probe to reproduce electrostatic interactions.

The results are given in Table 3 and Figure 5 a–d, and clearly show the prevalence of ionic and hydrophobic interactions, for amlodipine and lercanidipine, respectively. Figure 5 a–c show cubes and clusters obtained from the MIF with PO_4^{2-} as a probe (-5 kcal mol^{-1}) in dark grey, for amlodipine (Figure 5 a) and for lercanidipine (Figure 5 c). Figures 5 b (amlodipine) and 5 d (lercanidipine) give the same information using MIFs generated with the DRY probe (-0.3 kcal mol^{-1}). Beside the different extensions, dark grey zones are also located in different regions of the two investigated calcium channel blockers since they are close to the protonated nitrogen and are rather localized. Conversely, DRY cubes are more dispersed around the hydrophobic molecular moieties (e.g. aromatic rings). As expected, the cubes obtained with different MIFs for the different molecules cannot be superimposed. Taken together, these findings could be of great relevance in designing calcium channel blockers with ad hoc plasma half-life features.

Lercanidipine and amlodipine were built using Corina in their protonated form.[14,15] The same stereochemistry (*R*) was maintained for both compounds. The GRID NPLA parameter was set to 2, and the hydrophobic probe (DRY) and PO_4^{2-} probe were used.

New life for GRID

GRID was taken as an example of software that provides grid-based interaction energy maps. The choice of this application was intentional; we select a product that is solid from a theoretical point of view and well known to most medicinal chemists, even more so now because of work recently done by Molecular Discover as discussed below. It was also selected for its

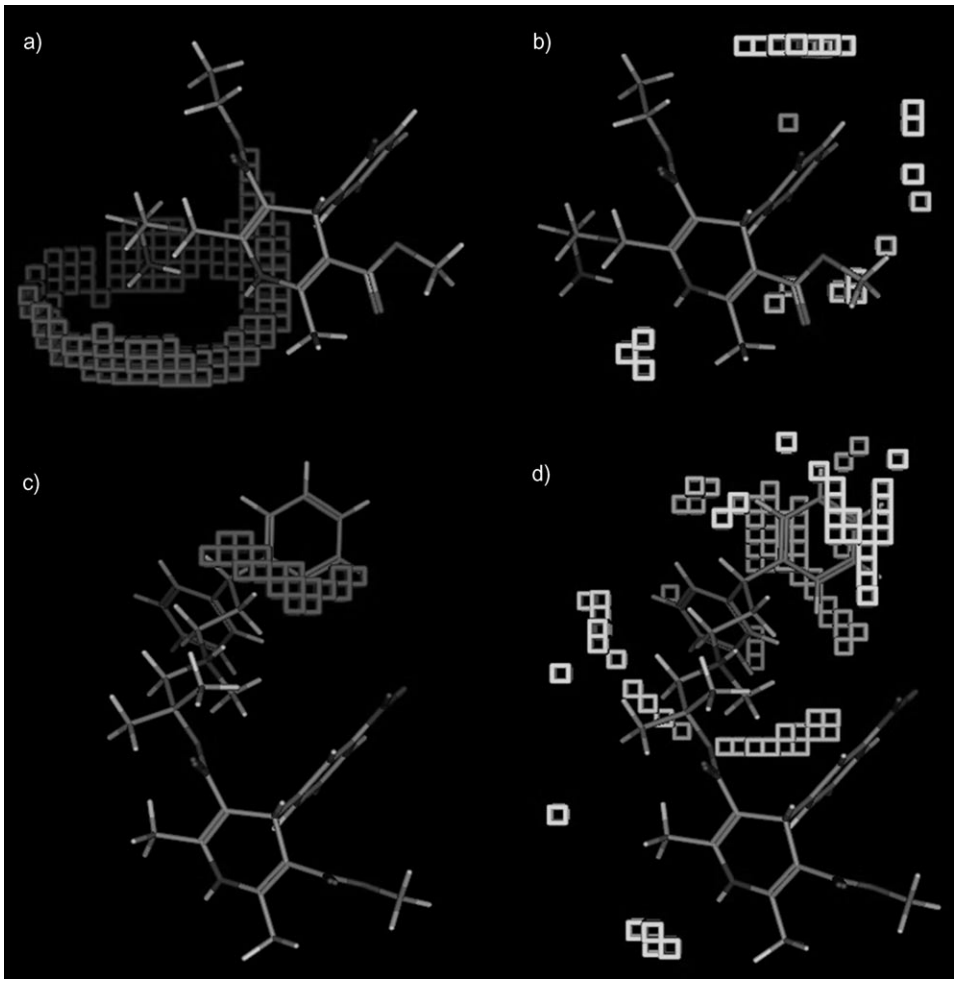

Figure 5. Results of the application of the GRID/BIOCUBE4mf procedure to Amlodipine and Lercanidipine, for ease of interpretation amlodipine and lercanidipine are shown in the same orientation. a) Amlodipine with cubes (dark grey) extracted from the MIF calculated using the PO_4^{2-} probe at -5 kcal mol^{-1}. b) Amlodipine with cubes (light grey) extracted from the MIF calculated using the DRY probe at -0.03 kcal mol^{-1}. c) Lercanidipine with cubes (dark grey) extracted from the MIF calculated using the PO_4^{2-} probe at -5 kcal mol^{-1}. d) Lercanidipine with cubes (light grey) extracted from the MIF calculated using the DRY probe at -0.03 kcal mol^{-1}.

of software, with a background that makes it accessible to most bioscientists. Nevertheless, it has largely fallen out of use in recent years, mainly because of the limited practical application of the results.

In 2002, two excellent commercially available software packages were released, designed to automatically extract the information present in MIFs in the form of numerical descriptors, which in turn can be used to generate 3D-QSAR models: VolSurf and Almond by Molecular Discovery.[23] Both pieces of software are extremely useful in providing fast and often accurate predictions of a given biological activity (e.g. log *P* prediction,[24] blood–brain permeation,[25] protein binding,[26] hERG blockade[27]) using chemometric strategies.

However, the VolSurf and ALMOND packages do not give an in-depth inspection of GRID results and moreover cannot be applied to small compound series or even single proteins, limiting the use of GRID in some ways. With BIOCUBE4mf, we extend the application of GRID and similar computational tools that are of huge potential interest in biosciences as shown by the examples discussed.

Table 3. Numerical output obtained from BIOCUBE4mf: Data obtained by BIOCUBE4 mf for amlodipine and lercanidipine

Compound	Probe PO_4^{2-} -5 kcal mol^{-1}		Probe DRY -0.3 kcal mol^{-1}	
	Cubes	*Clusters*	*Cubes*	*Clusters*
Amlodipine	198	24	40	15
Lercanidipine	25	5	97	39

application in describing surface protein[16–18] and pharmacokinetic[19–21] properties.

GRID was designed for investigating macromolecules and their interactions with small ligands, and takes into account all major pitfalls of this type of product,[22] namely the sophisticated treatment of electrostatics, ionization, conformational flexibility and the presence of water molecules in the protein–ligand interaction. For these reasons, GRID is a very solid piece

Conclusions

Even if chemists are culturally far from sharing information with other scientists working in neighboring fields, many computational tools developed for investigating chemical topics could easily be transferred and applied to biotopics, since biointeractions are governed by the laws of chemistry.

This paper describes a computational strategy for the extraction of the most information from grid-based interaction energy maps, and its application to biosciences through four selected examples. In particular, we show that BIOCUBE4mf, a simple application developed in our laboratories, coupled with GRID, could also be used by bioscientists to study proteins–ligand interactions.

The examples discussed highlight two situations that are particularly suitable for the application of the GRID/BIOCUBE4mf approach. The first concerns the design of active site ligands using the information obtained from the active site map

generated with BIOCUBE4mf. The second concerns the comparison of two proteins by means of their surface maps obtained using the GRID/BIOCUBE4mf approach. Following the completion of genome projects for a number of organisms, it is becoming evident that a relatively large proportion of the genes identified encode proteins that have no sequence homology with known proteins. One possible approach towards understanding protein function is to identify the proteins with which a particular protein associates. This could be facilitated by visual inspection of BIOCUBE4mf maps, and by using a comparison tool to express similarity in quantitative terms.

In summary, the computational strategy described represents an attempt to move chemistry towards biology, a step with the more general aim of establishing interdisciplinary networks of scientists, which can be seen as one of the biggest and most important challenges of future scientific research.

Acknowledgements

GE and GEC are indebted to the University of Turin for financial support. Thanks also go to Dr. Dario Longo (University of Turin) for testing the software.

Keywords: biocube4mf · grid · molecular interaction fields · molecular modeling · molecular recognition

[1] P. Murray-Rust, J. B. Mitchell, H. S. Rzepa, *BMC Bioinf.* **2005**, *6*, 141.
[2] M. Baker, *Nat. Rev. Drug Discovery* **2006**, *5*, 707–708 .
[3] G. Ermondi, G. Caron, *Biochem. Pharmacol.* **2006**, *72*, 1633–1645 .
[4] W. J. Geldenhuys, K. E. Gaasch, M. Watson, D. D. Allen, C. J. Van der Schyf, *Drug Discov. Today* **2006**, *11*, 127–132 .
[5] P. M. Dean in *3D QSAR in Drug Design* (Ed.: H.Kubinyi), ESCOM, Leiden, **1993**, pp. 150–172.
[6] C. J. Miller, J. L. Elliot, R. J. Collier, *Biochemistry* **1999**, *38*, 10432–10441 .
[7] C. Petosa, R. J. Collier, K. R. Klimpei, S. H. Leppia, R. C. Liddington, *Nature* **1997**, *385*, 833–838 .
[8] M. W. H. Coughtrie, *Pharmacogenomics J.* **2002**, *2*, 297–308.
[9] D. Bichet, M. Grabe, Y. N. Jan, L. Y. Jan, *Proc. Natl. Acad. Sci. USA* **2006**, *103*, 14355–14360.
[10] L. Herbette, M. Vecchiarelli, A. Leonardi, *J. Cardiovasc. Pharmacol.* **1997**, *29*, S19–24.
[11] T. F. Lüscher, F. Cosentino, *Drugs* **1998**, *55*, 509–517 .
[12] G. Caron, G. Ermondi in *Pharmacokinetic Profiling in Drug Research: Biological, Physicochemical and Computational Strategies* (Eds.: B. Testa, S. Kraemer, H. Wunderli-Allenspach, G. Folkers), VHCA, Zürich, **2006**, pp. 165–185.
[13] R. P. Mason, S. F. Campbell, S.-D. Wang, L. G. Herbette, *Mol. Pharmacol.* **1989**, *36*, 634–640.
[14] J. Gasteiger, CORINA **2004**; http://www2.chemie.uni-erlangen.de/software/corina/index. html.
[15] J. Gasteiger, C. Rudolph, J. Sadowski, *Tetrahedron Computer Methodology* **1990**, *3*, 537–547.
[16] E. Filipponi, V. Cecchetti, O. Tabarrini, D. Bonelli, A. Fravolini, *J. Comput. Aided Mol. Des.* **2000**, *14*, 277–291.
[17] T. Naumann, H. Matter, *J. Med. Chem.* **2002**, *45*, 2366–2378.
[18] M. Ridderstrom, I. Zamora, O. Fjellstrom, T. B. Andersson, *J. Med. Chem.* **2001**, *44*, 4072–4081.
[19] P. Crivori, G. Cruciani, P. A. Carrupt, B. Testa, *J. Med. Chem.* **2000**, *43*, 2204–2216.
[20] C. Koukoulitsa, G. Geromichalos, H. Skaltsa, *J. Comput. Aided Mol. Des.* **2005**, *19*, 617–623.
[21] G. Berellini, G. Cruciani, R. Mannhold, *J. Med. Chem.* **2005**, *48*, 4389–4399.
[22] G. Klebe, *Drug Discov. Today* **2006**, *11*, 580–594.
[23] *Molecular Interaction Fields. Applications in Drug Discovery and ADME Prediction* (Ed.: G.Cruciani), Wiley-VCH, Zürich, **2006**.
[24] G. Caron, G. Ermondi, *J. Med. Chem.* **2005**, *48*, 3269–3279.
[25] P. Crivori, G. Cruciani, P. A. Carrupt, B. Testa, *J. Med. Chem.* **2000**, *43*, 2204–2216.
[26] G. Cruciani, P. Crivori, P. A. Carrupt, B. Testa, *J. Mol. Struct. THEOCHEM* **2000**, *503*, 17–30.
[27] G. Cianchetta, Y. Li, J. Kang, D. Rampe, D. Fravolini, G. Cruciani, R. J. Vaz, *Bioorg. Med. Chem. Lett.* **2005**, *15*, 3637–3642.

Received: July 31, 2008
Revised: October 22, 2008
Published online on December 10, 2008

